Contribution from the Departments of Chemistry, University of Hong Kong, Hong Kong, and The Chinese University of Hong Kong, Shatin, New Territories, Hong Kong

Stabilization of High-Valent Transition-Metal Complexes with Macrocyclic Tertiary Amines. Reinvestigation of the Synthesis, Electrochemistry, and Spectroscopy of Osmium(III) Macrocyclic Amine Complexes and X-ray Crystal Structure of *trans*-$[Os^{III}(16\text{-TMC})Cl_2]ClO_4$ (16-TMC = 1,5,9,13-Tetramethyl-1,5,9,13-tetraazacyclohexadecane)

Chi-Ming Che,*[1a] Wing-Kin Cheng,[1a] Ting-Fong Lai,[1a] Chung-Kwong Poon,[1a] and Thomas C. W. Mak[1b]

Received May 29, 1986

Dropwise addition of an ethanolic solution of Na_2OsCl_6 to a refluxing ethanolic suspension of L and tin plates yielded *trans*-$[Os^{III}LCl_2]^+$ [L = 14aneN$_4$ (1,4,8,11-tetraazacyclotetradecane), 15aneN$_4$ (1,4,8,12-tetraazacyclopentadecane), 16aneN$_4$ (1,5,9,13-tetraazacyclohexadecane), teta (*meso*-5,5,7,12,12,14-hexamethyl-1,4,8,11-tetraazacyclotetradecane), 16-TMC (1,5,9,13-tetramethyl-1,5,9,13-tetraazacyclohexadecane)]. The UV-vis spectra of *trans*-$[Os^{III}LCl_2]^+$ exhibited two ligand-to-metal charge-transfer (LMCT) $p_\pi(Cl) \rightarrow d_\pi(Os)$ transition bands in the 250–280- and 280–310-nm regions. The LMCT transition energy for *trans*-$[Os^{III}LCl_2]^+$ varies with L = $(NH_3)_4$ > $(en)_2$ > 2,3,2-tet > 3,2,3-tet > 14aneN$_4$ > 15aneN$_4$ ~ 16aneN$_4$ > 16-TMC > teta (2,3,2-tet = 3,7-diazanonane-1,9-diamine; 3,2,3-tet = 4,7-diazadecane-1,10-diamine). In acetonitrile, reversible Os(III)/Os(II) couples were observed at potentials −1.6 to −1.3 V vs. the $Cp_2Fe^{+/0}$ couple. The $E_{1/2}$ value for *trans*-$[Os^{III}LCl_2]^+$ is relatively insensitive to the macrocyclic ring size and decreases from L = 14aneN$_4$ to L = teta. For Os(III) secondary amine complexes, the electrochemical oxidation of Os(III) to Os(IV) was irreversible. For *trans*-$[Os^{III}(16\text{-TMC})Cl_2]^+$, a reversible Os(IV)/Os(III) couple was found at 0.67 V vs. the $Cp_2Fe^{+/0}$ couple and 0.81 V vs. NHE in acetonitrile and 0.1 M HCl, respectively. *trans*-$[Os^{IV}(16\text{-TMC})Cl_2]^{2+}$ has been characterized spectroscopically with a $p_\pi(Cl) \rightarrow d_\pi[Os(IV)]$ transition at 365 nm. The structure of *trans*-$[Os^{III}(16\text{-TMC})Cl_2]ClO_4$ has been determined by X-ray crystallography: orthorhombic; space group *Pnma*; a = 14.982 (3), b = 11.036 (3), c = 13.586 (4) Å; V = 2246.3 (9) Å^3; Z = 4. The *N*-methyl groups of the 16-TMC ligand adopt a "two up" and "two down" configuration, and the two chloride ligands are trans to each other. The Os–N and Os–Cl distances are 2.263 (17) and 2.348 (1) Å, respectively.

Introduction

The chemistry of osmium macrocyclic amine complexes remains relatively unexplored in recent years despite the rich coordination chemistry found for the ruthenium analogues.[2] As an extension of our work on high-valent oxo complexes of ruthenium macrocyclic tertiary amines,[3] we have been interested in the analogous studies of osmium. In 1981, the synthesis of *trans*-dihalogeno(macrocyclic tetraamine)osmium(III) complexes utilizing Na_2OsCl_6 and NaH_2PO_2 as starting materials was reported.[4] However, this method was either unsuccessful or ineffective for the synthesis of osmium(III) complexes with macrocyclic tertiary amines. In an attempt to develop the chemistry off high-valent osmium oxo complexes,[5] we have reinvestigated the coordination chemistry of osmium with macrocyclic tetradentate amines. This paper describes a modified procedure for the synthesis of *trans*-dichloro(tetraamine)osmium(III) complexes, *trans*-$[OsLCl_2]^+$ where L = 14aneN$_4$ (1,4,8,11-tetraazacyclotetradecane), 15aneN$_4$ (1,4,8,12-tetraazacyclopentadecane), 16aneN$_4$ (1,5,9,13-tetraazacyclohexadecane), teta (*C-meso*-5,5,7,12,12,14-hexamethyl-1,4,8,11-tetraazacyclotetradecane), or 16-TMC (1,5,9,13-tetramethyl-1,5,9,13-tetraazacyclohexadecane) (Figure 1). The UV–vis spectroscopic features and electrochemistry of these osmium(III) complexes are discussed. *trans*-$[Os(16\text{-TMC})Cl_2]ClO_4$ has also been characterized by X-ray crystallography.

Experimental Section

Materials. Na_2OsCl_6 was purchased from Johnson and Matthey Co. Ltd. The macrocyclic amine ligands were prepared by the published methods.[6-8] All reagents and solvents used were of analytical grade. Absolute AR ethanol was employed in the synthesis. Acetonitrile (Mallinckrodt Chrom. AR) used for electrochemical studies was twice distilled over CaH_2 under argon.

***trans*-$[Os^{III}(16aneN_4)Cl_2]ClO_4$.** An ethanolic solution of 16aneN$_4$ (0.4 g in 150 mL) and finely divided tin plates (12 g) was refluxed with vigorous stirring for ca. 10 min. An ethanolic solution of Na_2OsCl_6 (0.5 g in 200 mL) was then added dropwise to the refluxing solution. The addition process took 4–5 h for completion, and the resulting reaction mixture was further refluxed for another 12 h. After refluxing, the solution was acidified with diluted HCl (2 M) and filtered hot. The filtrate was rotary evaporated to dryness. The yellowish brown residue was dissolved in hot HCl (2 M, 15 mL). Upon addition of excess $NaClO_4$, yellowish brown solids precipitated, which were collected and washed with ice-cold water and an ethanol–diethyl ether (1:5) mixture. The products obtained in this way were contaminated with some partially dehydrogenated products. The following purification procedure is necessary for pure *trans*-$[Os^{III}(16aneN_4)Cl_2]ClO_4$.

The crude yellowish brown residue obtained by the above procedure was dissovled in hot HCl (3 M, 30 mL). Several pieces of zinc were added while the solution was kept at ~80 °C. When the solution appeared *light brown*, it was filtered hot and excess $NaClO_4$ was added. On cooling, some light brown microcrystalline solids were deposited, which were collected and washed with ice-cold water. Yield: ~45%. Anal. Calcd for $OsC_{12}H_{28}N_4Cl_3O_4$: C, 24.5; N, 9.5; H, 4.8. Found: C, 24.3; N, 9.4; H, 4.6. IR (Nujol mull): ν(N–H) 3200 cm^{-1}.

***trans*-$[Os^{III}(teta)Cl_2]ClO_4$.** This was similarly prepared as described for *trans*-$[Os^{III}(16aneN_4)Cl_2]ClO_4$. Yield: ~30%. Anal. Calcd for $OsC_{16}H_{36}N_4Cl_3O_4$: C, 29.8; N, 8.7; H, 5.6; Cl, 16.5. Found: C, 29.3; N, 8.4; H, 5.3; Cl, 16.8. IR (Nujol mull): ν(N–H) 3200 cm^{-1}.

***trans*-$[Os^{III}(15aneN_4)Cl_2]ClO_4$ and *trans*-$[Os^{III}(14aneN_4)Cl_2]ClO_4$.** These two complexes were similarly prepared as described for *trans*-$[Os^{III}(16aneN_4)Cl_2]ClO_4$. Yield: 50–60%. They are characterized by comparing their IR and UV–vis spectroscopic data with reported values.[4]

***trans*-$[Os^{III}(16\text{-TMC})Cl_2]ClO_4$.** An ethanolic solution of Na_2OsCl_6 (0.5 g in 200 mL) was added dropwise to a refluxing and vigorously stirred ethanolic suspension of 16-TMC (0.5 g in 150 mL) and tin plates (12 g). The addition process took 5 h for completion, and the reaction mixture was further refluxed overnight. After refluxing, the solution was

(1) (a) University of Hong Kong. (b) The Chinese University of Hong Kong.
(2) (a) Poon, C.-K.; Che, C.-M. *J. Chem. Soc., Dalton Trans.* **1980**, 786. (b) Che, C.-M.; Kwong, S.-S.; Poon, C.-K. *Inorg. Chem.* **1985**, *24*, 1601. (c) Che, C.-M.; Kwong, S.-S.; Poon, C.-K.; Lai, T.-F; Mak, T. C. W. *Inorg. Chem.* **1985**, *24*, 1359.
(3) (a) Che, C.-M.; Wong, K.-Y.; Mak, T. C. W. *J. Chem. Soc., Chem. Commun.* **1985**, 988. (b) Che, C.-M.; Wong, K.-Y.; Poon, C.-K. *Inorg. Chem.* **1985**, *24*, 1797. (c) Che, C.-M.; Wong, K.-Y.; Mak, T. C. W. *J. Chem. Soc., Chem. Commun.* **1985**, 546.
(4) Poon, C.-K.; Che, C.-M.; Tang, T.-W. *J. Chem. Soc., Dalton Trans.* **1981**, 1697.
(5) Che, C.-M.; Cheng, W.-K. *J. Am. Chem. Soc.* **1986**, *108*, 4644.
(6) Hung, Y.; Martin, L. Y.; Jackels, S. C.; Tait, A. T.; Busch, D. H. *J. Am. Chem. Soc.* **1977**, *99*, 4029.
(7) Alock, N. W.; Curzon, E. H.; Moore, P.; Pierpoint, C. *J. Chem. Soc., Dalton Trans.* **1984**, 605.
(8) Tait, A. M.; Busch, D. H. *Inorg. Nucl. Chem. Lett.* **1972**, *8*, 491.

0020-1669/87/1326-1678$01.50/0

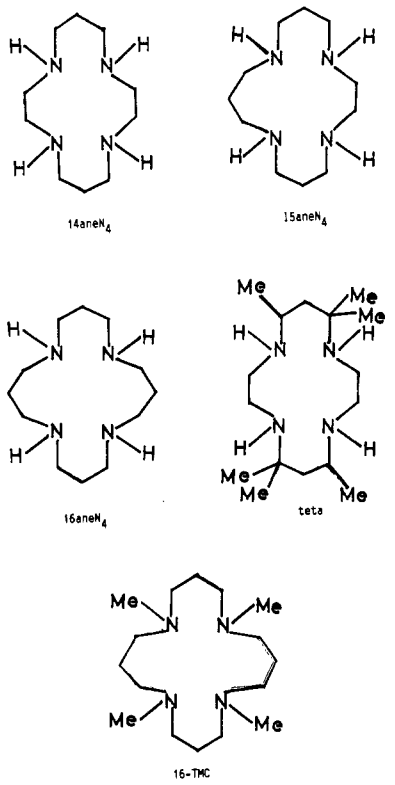

Figure 1. Structures of macrocyclic amines.

filtered and the filtrate was rotary evaporated to dryness. The yellow residue was dissolved in hot HCl (2 M, ca. 15 mL) and the resultant mixture filtered into a saturated solution of $NaClO_4$ (3 mL). Yellow *trans*-$[Os^{III}(16\text{-TMC})Cl_2]ClO_4$ precipitated. The product was recrystallized in hot HCl (1 M). Yield: ~40%. Anal. Calcd for $OsC_{16}H_{36}N_4Cl_3O_4$: C, 29.8; H, 5.6; N, 8.7; Cl, 16.5. Found: C, 29.7; H, 5.6; N, 8.4; Cl, 15.9. IR (Nujol mull): no ν(N–H) stretch in the 3000–3500-cm^{-1} region.

Physical Measurements. UV–vis electronic absorption spectra of the osmium(III) macrocyclic amine complexes were recorded on a Beckman Acta CIII UV–vis spectrophotometer. Infrared and far-infrared spectra were obtained as Nujol mulls on a Perkin-Elmer 577 spectrophotometer (4000–200 cm^{-1}). Cyclic voltammetric measurements were performed by using a PAR universal programmer (Model 175), potentiostat (Model 173), and digital coulometer (Model 179). Formal potentials were taken from the mean values of the cathodic and anodic peak potentials at 25 °C at a scan rate of 100 mV s^{-1}. Cyclic voltammograms were recorded either with a Houston 2000 XY recorder at slow scan rates (<500 mV s^{-1}) or with a Tektronix Model 5441 storage oscilloscope at fast scan rates (>500 mV s^{-1}). Pyrolytic graphite electrodes were used as working electrodes. All potential measurements were made against the Ag/$AgNO_3$ (0.1 M in CH_3CN) electrode. Controlled-potential electrolysis was performed by using a PAR coulometric cell system (Model 9610) equipped with a synchronous stirring motor (Model 377). A glassy carbon crucible was used as the working electrode. All reaction solutions were deaerated with argon gas before and during the constant-potential electrolysis. Electrolysis was conducted at a potential that was about 100 mV more positive than the formal potential of the osmium complex to be oxidized.

The changing UV–vis spectra during the oxidation of *trans*-$[Os^{III}(16\text{-TMC})Cl_2]^+$ were obtained by continually withdrawing samples from the solution undergoing constant-potental electrolysis and then recording their spectra.

Crystal Structure Determination of *trans*-$[Os^{III}(16\text{-TMC})Cl_2]ClO_4$. Crystal data for $OsC_{16}H_{36}N_4O_4Cl_3$: M_r = 645.04; orthorhombic; space group *Pnma*; a = 14.982 (3), b = 11.036 (3), c = 13.586 (4) Å; V = 2246.3 (9) Å^3; d_{measd} = 1.913 g cm^{-3}; Z = 4; d_{calcd} = 1.907 g cm^{-3}; μ(Mo Kα) = 60.73 cm^{-1}.

Intensity data (*hkl*; 1948 unique data, for which 1640 had $|F_o| > 3\sigma(|F_o|)$ were collected from a crystal of approximately 0.24 × 0.14 × 0.10 mm on a Nicolet R3m diffractometer with graphite-monochromatized Mo Kα radiation (λ = 0.71069 Å), by using the ω–2θ variable-scan (2.02–8.37° min^{-1}) technique in the bisecting mode up to $2\theta_{max}$ = 52°. Azimuthal scans of 20 selected strong reflections over a range of 2θ values were used to define a pseudoellipsoid for the application of absorption corrections (μr = 0.45; transmission factors 0.276–0.330).[9]

Table I. Fractional Coordinates[a] (×10^5 for Os; ×10^4 for Other Atoms in the Cation; ×10^3 for Atoms in ClO_4) and Thermal Parameters[b] (Å^2 × 10^4 for Os; Å^2 ×10^3 for Other Atoms) with Esd's in Parentheses

atom	x	y	z	U_{eq}/U
Os	14291 (6)	25000	13554 (6)	491 (2)*
Cl(1)	2659 (3)	2500	2427 (4)	77 (2)*
Cl(2)	188 (4)	2500	302 (4)	73 (2)*
N(1)	810 (7)	1036 (12)	2280 (9)	82 (4)*
N(2)	2077 (8)	1054 (13)	392 (10)	96 (5)*
C(1)	−81 (10)	640 (17)	1960 (13)	120 (6)*
C(2)	753 (13)	1380 (20)	3381 (12)	124 (8)*
C(3)	162 (17)	2500	3476 (22)	132 (11)*
C(4)	1387 (12)	−108 (15)	2319 (14)	117 (6)*
C(5)	1460	−790	1330	59
C(5′)	1600	−700	1280	59
C(6)	1493 (22)	−105 (30)	340 (22)	69 (7)
C(6′)	2411 (28)	−36 (39)	975 (27)	58 (8)
C(7)	2048 (19)	1417 (29)	−716 (22)	57 (6)
C(7′)	2985 (26)	1594 (37)	−22 (27)	52 (8)
C(8)	2768 (20)	2500	−828 (19)	134 (11)*
C(9)	2979 (18)	603 (27)	652 (20)	52 (5)
C(9′)	1573 (26)	651 (37)	−480 (28)	54 (8)
Cl(3)	75	250	635	52
O(1)	150	250	560	54
O(2)	120	250	725	95
O(3)	25	145	625	99
Cl(3′)	65	250	640	67
O(1′)	160	250	670	99
O(2′)	15	250	735	93
O(3′)	50	145	590	85

[a] Occupancy factors for partial atoms: C(5), C(6), C(7), C(9), 0.58 (3); C(5′), C(6′), C(7′), C(9′), 0.42 (3); Cl(3), O(1), O(2), O(3), 0.50; Cl(3′), O(1′), O(2′), O(3′), 0.50. [b] Asterisks indicate equivalent isotropic thermal parameters: $U_{eq} = {}^1/_3\sum_i\sum_j U_{ij}a_i^*a_j^*\mathbf{a}_i\mathbf{a}_j$. The exponent of the isotropic thermal parameters takes the form $-8\pi^2U(\sin^2\theta)/\lambda^2$.

Table II. Selected Bond Distances and Angles in *trans*-$[Os^{III}(16\text{-TMC})Cl_2]^+$

	(a) Distances, Å		
Os–Cl(1)	2.348 (5)	N(2)–C(6)	1.55 (3)
Os–Cl(2)	2.347 (5)	N(2)–C(6′)	1.52 (4)
Os–N(1)	2.246 (12)	N(2)–C(7)	1.56 (3)
Os–N(2)	2.281 (14)	N(2)–C(7′)	1.59 (4)
N(1)–C(1)	1.47 (2)	N(2)–C(9)	1.48 (3)
N(1)–C(2)	1.55 (2)	N(2)–C(9′)	1.47 (4)
N(1)–C(4)	1.53 (2)		
	(b) Angles, deg		
Cl(1)–Os–N(1)	88.7 (3)	N(1)–Os–N(2)	89.6 (5)
Cl(1)–Os–N(2)	91.2 (4)	N(1)–Os–N(1)[a]	92.0 (4)
Cl(2)–Os–N(1)	90.8 (3)	N(2)–Os–N(2)[a]	88.8 (5)
Cl(2)–Os–N(2)	89.3 (4)	Cl(1)–Os–Cl(2)	179.3 (2)

[a] Symmetry code: x, ${}^1/_2 - y$, z.

Structure Determination and Refinement. The structure was solved by Patterson and Fourier methods and refined by full-matrix least-squares techniques. The quantity minimized was $\sum w(F_o^2 - F_c^2)^2$, with weight $w = 1/\sigma^2(F_o^2)$. Atomic scattering factors were taken from ref 10, with anomalous dispersion corrections applied to those of osmium and chlorine.

During the early stage of refinement the carbon atoms C(6), C(7), and C(9) in the macrocycle and some of the oxygen atoms in the perchlorate ion showed abnormally large thermal motion; C(5), C(6), C(7), and C(9) were subsequently refined isotropically over two sites with initial site occupancy factors of 0.5. The position of the disordered perchlorate group was determined from difference maps. It was placed in two different sites, each with an occupancy factor of 0.5. All hydrogen atoms were omitted. In the final cycles of refinement, all non-hydrogen atoms

(9) Kofmann, G.; Huber, R. *Acta Crystallogr., Sect. A: Cryst. Phys., Diffr., Theor. Gen. Crystallogr.* **1968**, *24*, 348. North, A. C. T.; Phillips, D. C.; Mathews, F. S. *Ibid.* **1968**, *24*, 351.

(10) *International Tables for X-ray Crystallography*; Kynoch: Birmingham, England, 1974; Vol. 4, p 72.

Table III. Summary of Electronic Absorption Spectral Data of Dihalogeno(tetraamine)osmium(III) and -ruthenium(III) Complexes

complex	solvent	λ_{max}, nm[a]
trans-$[Os^{III}(NH_3)_4Cl_2]ClO_4$[b]	HCl (0.1 M)	271 (4810)
trans-$[Os^{III}(en)_2Cl_2]ClO_4$[c]	HCl (0.1 M)	284 (4360)
trans-$[Os^{III}(2,3,2\text{-tet})Cl_2]ClO_4$[c]	HCl (0.1 M)	291 (3840), 251 (1890)
trans-$[Os^{III}(3,2,3\text{-tet})Cl_2]ClO_4$[c]	HCl (0.1 M)	290 (3330), 254 (1920)
trans-$[Os^{III}(14aneN_4)Cl_2]ClO_4$[c,d]	CH_3CN	295 (3200), 263 (1290)
trans-$[Os^{III}(15aneN_4)Cl_2]ClO_4$[c,d]	CH_3CN	294 (3190), 262 (1130)
trans-$[Os^{III}(16aneN_4)Cl_2]ClO_4$[d]	CH_3CN	296 (2900), 268 (sh) (1000)
trans-$[Os^{III}(teta)Cl_2]ClO_4$[d]	CH_3CN	310 (2020), 268 (1220)
trans-$[Os^{III}(16\text{-TMC})Cl_2]ClO_4$[d]	CH_3CN	304 (3330), 276 (1040)
trans-$[Ru^{III}(en)_2Cl_2]ClO_4$[e]	HCl (0.1 M)	343 (3850)
trans-$[Ru^{III}(2,3,2\text{-tet})Cl_2]ClO_4$[e]	HCl (0.1 M)	349 (3430), 297 (1160)
trans-$[Ru^{III}(3,2,3\text{-tet})Cl_2]ClO_4$[e]	HCl (0.1 M)	351 (2560), 302 (1230)
trans-$[Ru^{III}(14aneN_4)Cl_2]ClO_4$[f]	H_2O	358 (2560), 315 (1230)
trans-$[Ru^{III}(15aneN_4)Cl_2]ClO_4$[f]	H_2O	359 (2410), 317 (1350)
trans-$[Ru^{III}(16aneN_4)Cl_2]ClO_4$[f]	H_2O	360 (2320), 318 (1320)
trans-$[Ru^{III}(teta)Cl_2]ClO_4$[e]	Me_2SO	382 (2270), 315 (1490)
trans-$[Ru^{III}(16\text{-TMC})Cl_2]ClO_4$[g]	HCl (0.1 M)	369 (2630), 320 (sh) (830)

[a] ϵ_{max} (cm^{-1} dm^3 mol^{-1}) in parentheses; sh = shoulder. [b] Reference 19. [c] Reference 5. [d] This work. [e] Reference 2a and 20. [f] Reference 18. [g] Reference 15.

in the cation, except the partial carbon atoms, were refined anisotropically and the parameters of the perchlorate group were not refined. The final R value is 0.058 for 1640 reflections with $|F_o| > 3\sigma|F_o|$. The goodness of fit $[\sum w(F_o^2 - F_c^2)^2/(m-p)]$ is 3.58 for 1640 measurements, m, and 110 parameters, p. All computations were performed by using the CRYM system.[11] Final atomic parameters of non-hydrogen atoms are listed in Table I. Selected bond distances and angles in the cation are listed in Table II. Listings of anisotropic thermal parameters and observed and calculated structure factors are available as supplementary material.

Results and Discussion

The modified procedure utilizing tin as the reducing agent appears to be an efficient method for the synthesis of osmium macrocyclic amine complexes. The previous method[4] gave very low yields of the product, with either sterically hindered tertiary amines or macrocycles of large ring size, such as $16aneN_4$. Occasionally, difficulties were encountered in reproducing the yields of the published procedure.[4] A major feature of the "improved synthesis" described here is the dropwise addition of the ethanolic solution of Na_2OsCl_6 to the refluxing ethanolic suspension of tin and amine. Under these conditions, a low-valent osmium complex that is reactive in metal-insertion reactions may be generated in situ. In general, the yield of osmium(III) complexes with secondary amines is usually higher than that with tertiary amines. As in the chemistry of iron and ruthenium amine complexes,[12,13] the coordinated primary or secondary amine easily undergoes facile intramolecular oxidative-dehydrogenation reactions.[4]

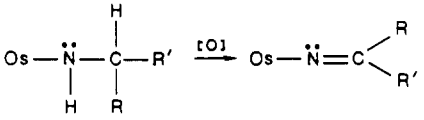

Thus, a reductive purification step, involving the treatment of the crude product with Zn/HCl, is necessary for obtaining pure osmium(III) secondary amine complexes such as *trans*-$[Os^{III}(teta)Cl_2]ClO_4$. In general, *trans*-$[Os^{III}LCl_2]ClO_4$ complexes are light yellow or brown and stable at room temperature. They are isomerically pure, as they exhibited only one band on a Dowex AG50W-X2 cation-exchange resin (eluted with 1 M HCl). For the secondary amine complexes such as *trans*-$[Os^{III}(teta)Cl_2]ClO_4$ and *trans*-$[Os^{III}(16aneN_4)Cl_2]ClO_4$, only one intense ν(N–H) stretch in the 3180–3200-cm^{-1} region is found in accord with their formulation as the trans isomers. As expected, the IR spectrum of *trans*-$[Os^{III}(14aneN_4)Cl_2]ClO_4$ displays a distinctive doublet and singlet in the 900- and 800-cm^{-1} regions, respectively,[4] which are characteristic features for *trans*-dihalo(cyclam)metal complexes (cyclam = $14aneN_4$).[14] The IR spectrum of *trans*-$[Os^{III}(16\text{-TMC})Cl_2]ClO_4$ is virtually identical with that of its ruthenium analogue.[15] *trans*-$[Os^{III}(14aneN_4)Cl_2]ClO_4$[16] and *trans*-$[Os^{III}(16\text{-TMC})Cl_2]ClO_4$ have been characterized by X-ray crystallography, with the structure of the latter species described later in the text.

Description of the Structure. There has been no structural work reported on osmium macrocyclic amine complexes. Figure 2 shows the ORTEP drawings of the two possible conformations of the cation and the atomic numbering system. The Os, Cl(1), Cl(2), C(3), C(8), Cl(3), Cl(3′), O(1), O(1′), O(2), and O(2′) atoms all lie on the crystallographic mirror plane. The chloride ligands are trans to each other, and the cation has an octahedral configuration. The six-membered chelate rings are in chair conformations. In one conformation of the cation (Figure 2a), the N-methyl groups of the 16-TMC ligand assume a "two up" or "two down" configuration, as in the case of *trans*-$[Ru^{VI}(16\text{-TMC})O_2]^{2+}$.[17] In the other one (Figure 2b), the four N-methyl groups orient themselves in the same direction, that is a "four up" or down" configuration. Unlike *trans*-$[Ru^{III}(14aneN_4)Cl_2]^+$,[18] where non-bonded interactions between Ru–Cl and N–H groups were found, the Cl–Os–Cl axis is essentially perpendicular to the equatorial plane (Cl(1)–Os–Cl(2) = 179.3 (2)°). The measured Os–Cl and Os–N distances of 2.348 (1) and 2.263 (17) Å, respectively, are necessarily longer than those of the ruthenium analogues (Ru–Cl and Ru–N distances are 2.343 (1) and 2.083 (3) Å, respectively, in *trans*-$[Ru^{III}(14aneN_4)Cl_2]^+$).[18,20] The bond angles and distances of the 16-TMC ligand are normal.[7,17] The average Cl–O distance and O–Cl–O angle in the perchlorate group are respectively 1.44 ± 0.03 Å and 109 ± 1°.

Electronic Spectra of Osmium(III) Macrocyclic Amine Complexes. Table III summarizes the UV–vis spectral data for the dichloro(tetraamine)osmium(III) complexes and the ruthenium analogues. The electronic spectra of *trans*-$[Os^{III}LCl_2]^+$ (L = macrocyclic tetradentate amines) are similar to those of the ruthenium analogues except that the ligand-to-metal charge-transfer (LMCT) transitions, $p_\pi(Cl) \rightarrow d_\pi(M)$ (M = Ru or Os) are blue-shifted from ruthenium to osmium. A single Laporte-allowed transition $[p_\pi(Cl) \rightarrow d_\pi(Os)]$ at 270 nm is observed for *trans*-$[Os(NH_3)_4Cl_2]^+$.[19] For the *trans*-$[Os^{III}LCl_2]^+$ system, two LMCT

(11) CRYM system of crystallographic programs developed by R. E. Marsh and co-workers at the California Institute of Technology, 1984.
(12) Poon, C.-K.; Che, C.-M. *J. Chem. Soc., Dalton Trans.* **1981**, 1019.
(13) Dabrowiak, J. C.; Busch, D. H. *Inorg. Chem.* **1975**, *14*, 1881.
(14) Poon, C.-K. *Inorg. Chim. Acta* **1971**, *5*, 322.
(15) Che, C.-M.; Wong, K.-Y.; Poon, C.-K. *Inorg. Chem.* **1986**, *25*, 1809.
(16) X-ray structure of *trans*-$[Os^{III}(14aneN_4)Cl_2]ClO_4$: Che, C.-M.; Poon, C.-K., unpublished results.
(17) Mak, T. C. W.; Che, C.-M.; Wong, K.-Y. *J. Chem. Soc., Chem. Commun.* **1985**, 986.
(18) Walker, D. D.; Taube, H. *Inorg. Chem.* **1981**, *20*, 2828.
(19) Buhr, J. D.; Winkler, J. R.; Taube, H. *Inorg. Chem.* **1980**, *19*, 2416.
(20) Poon, C.-K.; Lau, T.-C.; Che, C.-M. *Inorg. Chem.* **1983**, *22*, 3893.

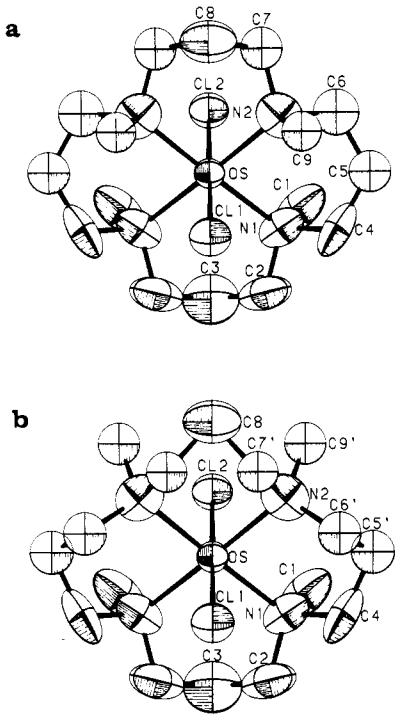

Figure 2. ORTEP drawings of the two possible conformations of the *trans*-$[Os^{III}(16\text{-TMC})Cl_2]^+$ cation, (a) "two up" or "two down" and (b) "four up" or "four down" configurations.

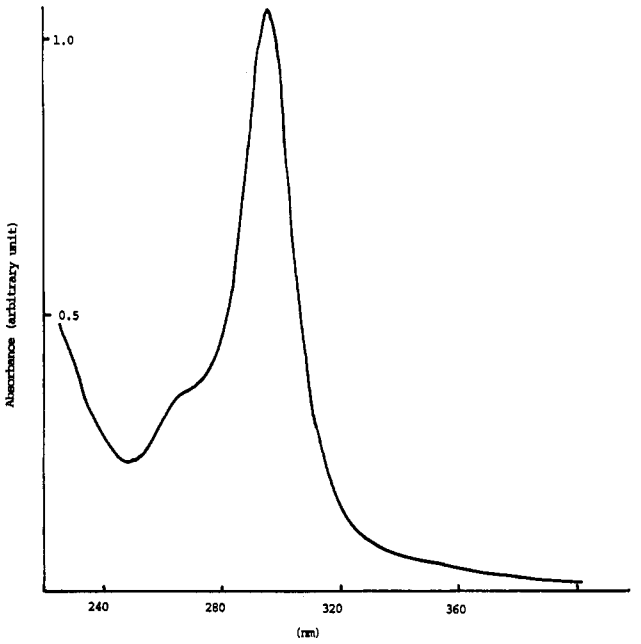

Figure 3. UV–vis absorption spectrum of *trans*-$[Os^{III}(16\text{-TMC})Cl_2]^+$ in acetonitrile.

bands at 250–280 and 290–310 nm, with the latter one more intense than the former, are observed. The UV–vis spectrum of *trans*-$[Os^{III}(16\text{-TMC})Cl_2]^+$ is shown in Figure 3. Walker and Taube[18] showed that the interaction between chloride ligands and the hydrogen atoms attached to the nitrogen of the macrocyclic secondary amine will split the degeneracy of the chloride p_π levels, producing two Laporte-allowed transitions (Figure 4). This would also be the case for the osmium(III) macrocyclic amine complexes, and we assigned the two LMCT bands as the $b_u \rightarrow b_g^*$ and $a_u \rightarrow b_g^*$ transitions. The splitting of the p_π levels in the osmium(III) complex (for example, 4120 cm^{-1} in *trans*-$[Os^{III}(14aneN_4)Cl_2]^+$) is larger than that for its ruthenium analogue (for example, 3500 cm^{-1} in *trans*-$[Ru^{III}(14aneN_4)Cl_2]^+$.[18,20] The energy of the lowest $p_\pi(Cl) \rightarrow d_\pi(Os)$ transition for *trans*-$[Os^{III}LCl_2]^+$ decreases in

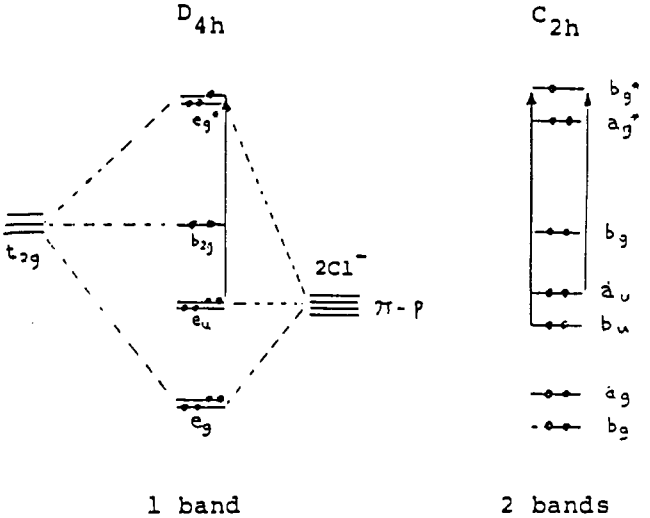

Figure 4. Simplified molecular orbital diagram for osmium(III) complexes.

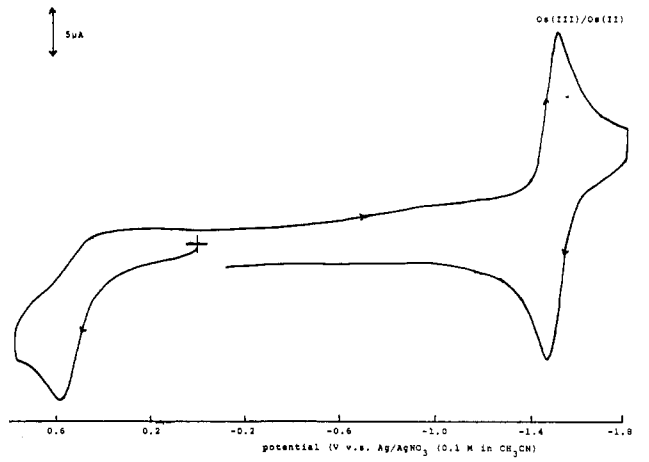

Figure 5. Cyclic voltammogram of *trans*-$[Os^{III}(14aneN_4)Cl_2]ClO_4$ in acetonitrile (supporting electrolyte 0.1 M $[Bu_4N]BF_4$; working electrode pyrolytic graphite; scan rate 100 mV s^{-1}).

the order L = $(NH_3)_4$ > $(en)_2$ > 2,3,2-tet > 3,2,3-tet > $14aneN_4$ ~ $15aneN_4$ > $16aneN_4$ > 16-TMC > teta (Table III). Similar findings for *trans*-$[Ru^{III}LCl_2]^+$ have also been observed.[20] The macrocyclic ring size has little effect on the LMCT transition of the *trans*-$[MLCl_2]^+$ (M = Ru and Os) system, and this is understandable because the electronic transition occurs within the nonbonding p_π and d_π levels. Previous works[20] suggested that the variation in the $p_\pi(Cl) \rightarrow d_\pi(M)$ transition energy from *trans*-$[M^{III}(14aneN_4)Cl_2]^+$ to *trans*-$[M^{III}(teta)Cl_2]^+$ (M = Ru and Os) could be explained in terms of a slight elongation of the M–Cl bond by the increase in steric constraints with the chelate ligand. This is expected to cause a red shift in the LMCT transition energy because decreasing overlap would result in a similar destabilization of the d_π^* (acceptor) orbitals. However, it is also likely that as the chloride ligand moves away from the metal center, it comes into greater contact with the solvent, causing the $p_\pi(Cl)$ levels to become more stable because of the solvation phenomena.[21]

Electrochemistry of Osmium(III) and Osmium(IV) Macrocyclic Amine Complexes. The cyclic voltammograms of *trans*-$[Os^{III}(14aneN_4)Cl_2]ClO_4$ and *trans*-$[Os^{III}(16\text{-TMC})Cl_2]ClO_4$ in CH_3CN are shown in Figures 5 and 6, respectively. For *trans*-$[Os^{III}LCl_2]ClO_4$, a reversible one-electron couple, corresponding to the reduction of Os(III) to Os(II), is found at the potential range of −1.6 to −1.2 V vs. the $Cp_2Fe^{+/0}$ couple (Table IV). In all of the complexes studied, the peak-to-peak separation

(21) *Inorganic Electronic Spectroscopy*, 2nd ed.; Lever, A. B. P., Ed.; Elsevier: New York, 1984; pp 332–334.

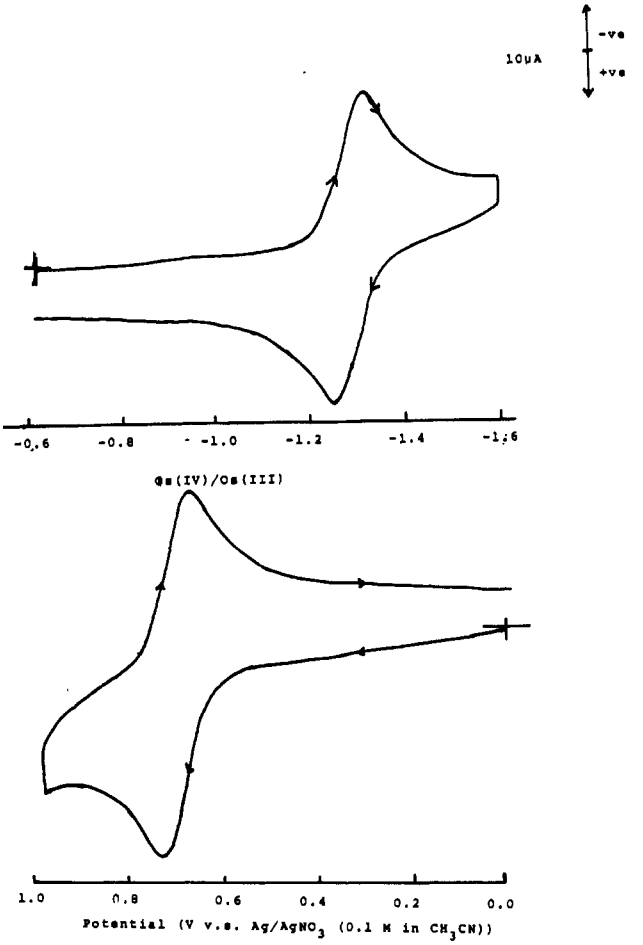

Figure 6. Cyclic voltammogram of *trans*-$[Os^{III}(16\text{-TMC})Cl_2]ClO_4$ in acetonitrile (supporting electrolyte 0.1 M $[Bu_4N]BF_4$; working electrode pyrolytic graphite; scan rate 100 mV s^{-1}).

Table IV. Potential Data for Os(III) and Ru(III) Complexes in Acetonitrile (Supporting Electrolyte 0.1 M $[Bu_4N]BF_4$)

complex	$E_{1/2}$, V vs. $Cp_2Fe^{+/0}$ couple[a] III/II	IV/III
trans-$[Os^{III}(14aneN_4)Cl_2]^+$	−1.55	0.54[b]
trans-$[Os^{III}(15aneN_4)Cl_2]^+$	−1.48	0.56[b]
trans-$[Os^{III}(16aneN_4)Cl_2]^+$	−1.44	0.60[b]
trans-$[Os^{III}(teta)Cl_2]^+$	−1.36	0.57[b]
trans-$[Os^{III}(16\text{-TMC})Cl_2]^+$	−1.31	0.67
trans-$[Ru^{III}(14aneN_4)Cl_2]^+$[c]	−0.94	1.34[b]
trans-$[Ru^{III}(teta)Cl_2]^+$[c]	−0.71	1.30[b]
trans-$[Ru^{III}(16\text{-TMC})Cl_2]^+$[c]	−0.54	1.22

[a] The half-wave potential $E_{1/2} = (E_{pc} + E_{pa})/2$ at 25 °C for reversible couples. For the irreversible wave, the anodic peak potential is measured at a scan rate of 100 mV s^{-1} at 25 °C. The $Cp_2Fe^{+/0}$ couple was found at 0.06 V vs. $Ag/AgNO_3$ (0.1 M in CH_3CN). [b] Irreversible wave. [c] Reference 15.

($\Delta E_p \sim 60$–70 mV) and current function ($i_{pa}/i_{pc} = 1$) for this couple are independent of scan rates (50–200 mV s^{-1}), indicating that the electrochemical reaction is at least quasi-reversible. The formal potentials ($E_{1/2}$) for *trans*-$[OsLCl_2]^{+/0}$ couples (Table IV) increase with L = $14aneN_4$ < $15aneN_4$ ~ $16aneN_4$ < teta < 16-TMC; similar findings for the ruthenium complexes have previously been reported.[15,22] We attributed the variation in the $E_{1/2}$ value with the nature of L as mainly due to the solvation phenomena.[22] In both Os(III) and Ru(II) complexes the macrocyclic ring size of L does not affect the $E_{1/2}$ value, and this is understandable, since the electron-transfer process between the low-spin d^5 (t_{2g}^5) and d^6 (t_{2g}^6) complexes occurs within the nonbonding d_π levels.

(22) Poon, C.-K.; Kwong, S.-S.; Che, C.-M.; Kan, Y.-P. *J. Chem. Sc., Dalton Trans.* **1981**, 1019.

Table V. Summary of Cyclic Voltammetric Data for the Oxidation of *trans*-$[Os^{III}(16\text{-TMC})Cl_2]ClO_4$ (1 mM) in Acetonitrile (Supporting Electrolyte 0.1 M $[Bu_4N]BF_4$)

scan rate, mV s^{-1}	i_{pa}, μA	$i_{pa}/\nu^{1/2}$	E_{pa}, V[b]	E_{pc}, V[b]	ΔE_p, mV	i_{pc}/i_{pc}[a]
10	10.4	3.32	+0.653	+0.583	70	0.78
20	14.6	3.27	+0.653	+0.583	70	0.82
50	22.5	3.18	+0.653	+0.583	70	0.95
100	33.0	3.20	+0.663	+0.583	80	0.96
200	46.3	3.27	+0.668	+0.578	90	0.96
500	74.3	3.32	+0.674	+0.582	92	0.99
1000	108.0	3.20	+0.674	+0.582	92	0.92
2000	136.5	3.06	+0.679	+0.575	105	0.98
5000	233.7	3.28	+0.696	+0.553	143	0.96

[a] i_{pc}/i_{pa} was calculated by using the empirical formula of Nicholson: *Anal. Chem.* **1965**, *37*, 1351. [b] Vs. $Cp_2Fe^{+/0}$ couple.

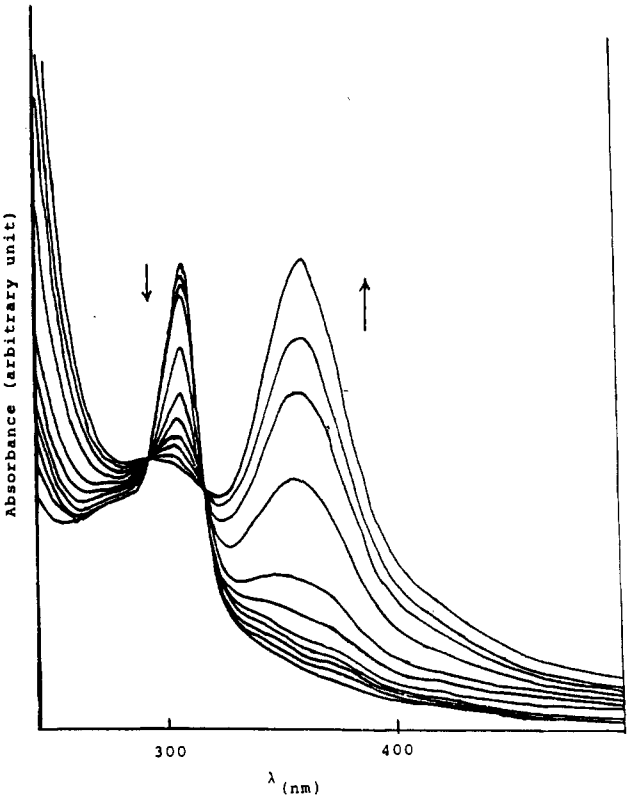

Figure 7. UV–vis spectral changes for the electrochemical oxidation of *trans*-$[Os^{III}(16\text{-TMC})Cl_2]^+$ to *trans*-$[Os^{IV}(16\text{-TMC})Cl_2]^{2+}$ in acetonitrile.

All osmium(III) secondary amine complexes display irreversible oxidative waves in the potential range of 0.55–0.60 V vs. the $Cp_2Fe^{+/0}$ couple (Figure 5). We argue that the electrochemically generated Os(IV) species is strongly oxidizing and oxidizes the coordinated amine (–NH—CHR) to an imine (–N=CR) group. Similar electrochemical behavior for *trans*-$[Ru^{III}(14aneN_4)Cl_2]ClO_4$ has previously been reported.[15] An outstanding feature of the electrochemistry of *trans*-$[Os^{III}(16\text{-TMC})Cl_2]^+$ in CH_3CN is the presence of a reversible Os(IV)/Os(III) couple at 0.67 V vs. the $Cp_2Fe^{+/0}$ couple (Figure 6). Table V summarizes the electrochemical data for the oxidation of *trans*-$[Os^{III}(16\text{-TMC})Cl_2]^+$ to *trans*-$[Os^{IV}(16\text{-TMC})Cl_2]^{2+}$. At a scan rate greater than 20 mV s^{-1}, ΔE_p widens while the current function ($i_{pa}/\nu^{1/2}$) and the current ratio ($i_{pc}/i_{pa} \approx 1$) remain constant, indicating that the electrochemical reaction is quasi-reversible. However, controlled-potential oxidation of *trans*-$[Os^{III}(16\text{-TMC})Cl_2]^+$ in acetonitrile at 0.80 V vs. the $Cp_2Fe^{+/0}$ couple revealed that the

oxidative current did not decay to the background level after 1 coulomb equiv needed for the complete oxidation of a one-electron process had been passed. The UV-vis spectral changes during the constant-potential electrolysis experiment are shown in Figure 7. Nice isosbestic points were maintained throughout the electrolysis reaction. The 306-nm band ($p_\pi(Cl) \rightarrow d_\pi(Os(III))$ gradually disappeared, and a new band at 365 nm developed. This 365-nm species would be immediately reconverted to the starting species *trans*-$[Os^{III}(16\text{-}TMC)Cl_2]^+$ upon addition of ascorbic acid (over 95% yield), indicating that it does not come from the degradative side reactions. We attributed the 365-nm band to be the $p_\pi(Cl) \rightarrow d_\pi(Os(IV))$ LMCT transition of *trans*-$[Os^{IV}(16\text{-}TMC)Cl_2]^{2+}$; similar findings for *trans*-$[Os^{IV}(NH_3)_4Cl_2]^{2+}$ ($\lambda_{max} \sim 357$ nm) have previously been reported.[19] The observed blue shift in the $p_\pi(Cl) \rightarrow d_\pi(M)$ transition from Ru(IV) (λ_{max} for *trans*-$[Ru^{IV}(16\text{-}TMC)Cl_2]^{2+}$ is ~410 nm)[15] to Os(IV) is in parallel with the corresponding decrease in the formal potential of the M(IV)/M(III) couple. The differences in the $E_{1/2}$ values between Ru and Os are 430 and 830 mV for the *trans*-$[M(16\text{-}TMC)Cl_2]^{2+/+}$ and *trans*-$[M(16\text{-}TMC)Cl_2]^{+/0}$ couples, respectively. The results suggest that the effect of replacing the metal (Ru with Os) on the reduction potential of the metal complex is more prominent in the trivalent [M(III)] than the tetravalent [M(IV)] state.

The electrochemistry of *trans*-$[Os^{III}(16\text{-}TMC)Cl_2]^+$ has also been studied in an aqueous medium. In 0.1 M HCl, the Os(IV)/Os(III) couple is fully reversible ($E_{1/2} = 0.81$ V vs. NHE) with $\Delta E_p = 60$-70 mV and $i_{pc}/i_{pa} = 1$. At pH 7, the electrochemical oxidation is less reversible but the Os(IV)/Os(III) couple still exists with $i_{pc}/i_{pa} = 0.73$ at a scan rate of 50 mV s^{-1}. The finding is different from Taube's work[19] where the electrochemical oxidation of *trans*-$[Os^{III}(NH_3)_4Cl_2]^+$ to *trans*-$[Os^{IV}(NH_3)_4Cl_2]^{2+}$ is completely irreversible at pH 7.6. The instability of *trans*-$[Os^{IV}(NH_3)_4Cl_2]^{2+}$ has been attributed to the oxidative deprotonation reaction of $Os\text{-}NH_3$ in a high-pH medium. *The usefulness of saturated macrocyclic tertiary amines in the stabilization of highly oxidizing transition-metal complexes is once again illustrated here.* The possibility of developing stable but strongly oxidizing osmium complexes for uses in oxidative reactions is under active investigation in our laboratories.

Acknowledgment. We acknowledge support from the Committee on Research and Conference Grants of the University of Hong Kong (C.-M.C., W.-K.C., and C.-K.P.). W.-K.C. is a Croucher Studentship holder (1984-1987).

Supplementary Material Available: A table of anisotropic thermal parameters (1 page); a listing of calculated and observed structure factors (5 pages).

Contribution from the Department of Chemistry,
The University of Western Ontario, London, Ontario N6A 5B7, Canada

Syntheses of $(Me_4N)_2[(\mu\text{-}EPh)_6(MX)_4]$ (M = Cd, Zn; E = S, Se; X = Cl, Br, I). Crystal and Molecular Structures of $(Me_4N)_2[(\mu\text{-}EPh)_6(CdBr)_4]$ (E = S, Se) and Characterization of $[(\mu\text{-}EPh)_6(CdX)_4]^{2-}$ in Solution by ^{113}Cd and ^{77}Se NMR

Philip A. W. Dean,* Jagadese J. Vittal, and Nicholas C. Payne*

Received September 18, 1986

The direct, quantitative reaction of the adamantanoid anions $[(\mu\text{-}EPh)_6(MEPh)_4]^{2-}$ (M = Cd, Zn; E = S, Se) with X_2 (X = Cl, Br, I) in acetone or MeCN or, for X = Cl, $PhICl_2$ in MeCN, provides a simple route to the new complexes $[M_4(EPh)_6X_4]^{2-}$ isolated as Me_4N^+ salts in high yield. The structurally representative salts $(Me_4N)_2[Cd_4(EPh)_6Br_4]$ (E = S, Se) have been fully characterized by single-crystal X-ray diffractometry techniques. Both crystallize in the cubic space group $P2_13$ with four formula units in the cell. The dimensions are $a = 17.869$ (2) Å for $(Me_4N)_2[Cd_4(SPh)_6Br_4]$ (**1**) and $a = 18.062$ (2) Å for $(Me_4N)_2[Cd_4(SePh)_6Br_4]$ (**2**). The structures have been refined by full-matrix least-squares techniques on F to agreement factors $R = 0.033$ (1343 observations with $F_o > 5\sigma(F_o)$) for **1** and $R = 0.033$ (989 observations with $F_o > 5\sigma(F_o)$) for **2**. In each salt, both cations and anions lie on a crystallographic threefold axis. In the chiral $[(\mu\text{-}EPh)_6(CdBr)_4]$ anions in **1** and **2**, the $Cd_4E_6Br_4$ core consists of a Cd_4 tetrahedron, regular within experimental error, inscribed in a slightly irregular octahedron defined by the bridging E atoms in an adamantanoid cage. Each Cd atom is tetrahedrally coordinated by one terminal Br and three bridging E atoms. The average Cd···Cd distance is 4.166 (3) for **1** and 4.251 (6) Å for **2**, the Cd-Br distances are 2.559 (3) and 2.565 (2) Å for **1** and 2.568 (4) and 2.581 (2) Å for **2**, the Cd-S distances are in the range 2.541 (3)-2.554 (3) Å for **1**, and the Cd-Se distances are in the range 2.627 (2)-2.654 (2) Å for **2**. The anions in **1** and **2** represent the first examples containing the $M_4(\mu\text{-}EPh)_6$ core in which the axial/equatorial dispositions of the EPh groups in the tetracyclic structure are aaa,aee,aee,aee. The absolute structures of **1** and **2** have been determined by measurement of Bijvoet pairs. NMR (^{113}Cd, ^{77}Se) studies of $[Cd_4(EPh)_6X_4]^{2-}$ show the persistence of fully terminally halogen substituted tetranuclear structures in solution. At reduced temperatures, exchange of both chalcogenates and halogens between clusters is slow on the NMR time scale. In addition, a slow-exchange ^{77}Se NMR spectrum has been observed for $[(\mu\text{-}SePh)_6(CdSePh)_4]^{2-}$.

Introduction

Recent advances in the chemistry of metalloproteins have stimulated interest in the fundamental coordination chemistry of simple metal thiolate complexes.[1-6] Frequently encountered among such complexes is the adamantane-like cage structure, with a tetrahedrally disposed set of metal atoms and an octahedrally disposed core of bridging sulfur atoms giving overall (idealized) T_d symmetry. This structural type has been established for the thiolate complexes $[(\mu\text{-}SR)_6Cu_4]^{2-}$ (R = Me, Ph)[2] and $[(\mu\text{-}SPh)_6(MSPh)_4]^{2-}$ (M = Mn(II),[3] Fe(II),[4] Co(II),[5] Cd(II),[6] Zn-

(1) (a) Dance, I. G. *Polyhedron* **1986**, *5*, 1037 and references therein. (b) Ibers, J. A.; Holm, R. H. *Science (Washington, D.C.)* **1980**, *209*, 223. (c) Watson, A. D.; Rao, Ch. P.; Dorfman, J. R.; Holm, R. H. *Inorg. Chem.* **1985**, *24*, 2820 and references therein.

(2) (a) Coucouvanis, D.; Murphy, C. N.; Kanodia, S. K. *Inorg. Chem.* **1980**, *19*, 2993. (b) Dance, I. G.; Bowmaker, G. A.; Clark, R. G.; Seadon, J. K. *Polyhedron* **1983**, *2*, 1031. (c) Dance, I. G.; Calabrese, J. C. *Inorg. Chim. Acta* **1976**, *19*, L41. (d) Nicholson, J. R.; Abrahams, I. L.; Clegg, W.; Garner, C. D. *Inorg. Chem.* **1985**, *24*, 1092.

(3) Costa, T.; Dorfman, J. R.; Hagen, K. S.; Holm, R. H. *Inorg. Chem.* **1983**, *22*, 4091.

(4) Hagen, K. S.; Stephan, D. W.; Holm, R. H. *Inorg. Chem.* **1982**, *21*, 3928.

(5) (a) Dance, I. G. *J. Am. Chem. Soc.* **1979**, *101*, 6264. (b) Dance, I. G.; Calabrese, J. C. *J. Chem. Soc., Chem. Commun.* **1975**, 762.

(6) Hagen, K. S.; Holm, R. H. *Inorg. Chem.* **1983**, *22*, 3171.

0020-1669/87/1326-1683$01.50/0